

Reliability Based Design Using Variable Fidelity Optimization

Shawn E. Gano* Harish Agarwal† John E. Renaud ‡
University of Notre Dame, Notre Dame, Indiana, 46556-5637, U.S.A.

Andrés Tovar§
Universidad Nacional de Colombia, Bogotá, Colombia

Competitive marketplaces have driven the need for simulation based design optimization to produce efficient and cost effective designs. However, such design practices are typically deterministic and don't take into account model uncertainties or manufacturing tolerances. Deterministic designs may lie on failure driven constraints, resulting in designs characterized by a high probability of failure. Reliability based design optimization (RBDO) methods have been developed to obtain designs that optimize a merit function while ensuring a target reliability level. Unfortunately, these methods are notorious for the high computational expense they require to converge. There has been a considerable effort to reduce the computational cost, many of these methods have used approximations which are not guaranteed to converge to the optimal solution of the original high fidelity problem. In this research variable fidelity methods are used to reduce the cost of RBDO. Variable fidelity methods use a set of models with varying degrees of fidelity and computational expense to reduce the cost of optimization. The variable fidelity RBDO methodology developed in this investigation is demonstrated on two test cases: a nonlinear analytic problem and a high-lift airfoil design problem. For each of these problems the proposed method shows considerable savings for performing RBDO as compared with standard approaches.

Nomenclature

$\beta()$	Multiplicative scaling function
β_i	Reliability index of the i^{th} failure mode
Δ	Trust region size
ϵ_f	Objective function convergence tolerance
ϵ_x	Design variable convergence tolerance
γ	Additive scaling function
\mathbf{g}^{rc}	Reliability inequality constraints
\mathbf{U}	Standard normal random variables
\mathbf{V}	Vector of random variables
η	Limit state parameters
θ	Distribution parameters of the random variables \mathbf{V}
\mathbf{g}^D	Deterministic constraints
\mathbf{g}^R	Failure drive or probabilistic constraints
\mathbf{p}	Parameters that are fixed in the design problem

*Ph.D. Candidate, Aerospace and Mechanical Engineering, sgano@nd.edu, Student Member AIAA.

†Ph.D. Candidate, Aerospace and Mechanical Engineering, hagarwal@nd.edu, Student Member AIAA.

‡Professor, Aerospace and Mechanical Engineering, John.E.Renaud.2@nd.edu, Associate Fellow AIAA.

§Assistant Professor, Department of Mechanical and Mechatronic Engineering, atovar@unal.edu.co, Member AIAA.

Copyright © 2005 by John E. Renaud. Published by the American Institute of Aeronautics and Astronautics, Inc. with permission.

\mathbf{v}	Realization of the random variables \mathbf{V}
\mathbf{x}	Design vector
\mathbf{x}^l	Lower bound of the design vector
\mathbf{x}^u	Upper bound of the design vector
\mathcal{W}	Hybrid weighting value
∇	Gradient operator
∇^2	Hessian operator
ρ	Trust region ratio
c_d	Sectional drag coefficient
c_l	Sectional lift coefficient
c_m	Sectional moment coefficient about the aerodynamic center
f	Objective or merit function
$f_{\mathbf{V}}(\mathbf{v})$	Joint probability density function (PDF) of \mathbf{V}
N_D	Number of deterministic constraints
N_R	Number of failure driven or probabilistic constraints
P	Probability of failure

Subscripts

m	Number of design variables
n	Current iteration number
<i>scaled</i>	Scaled low fidelity value
t	Target value

Superscripts

\sim	Approximate function
T	Transpose operator

I. Introduction

DESIGNS produced by deterministic optimization are often on the boundary of one or more constraints. Such designs leave no room for uncertainties such as those that may arise out of manufacturing tolerances, material property variations, or the unpredictability of external forces and loadings which may result in catastrophic failure. To address this issue engineers have typically used worst case values for the uncertain parameters; this leads to unnecessarily conservative designs. These designs are more expensive, where expense is paramount in a competitive marketplace. Furthermore, to address unknown failure modes safety factors have been traditionally used to further increase the robustness of designs. The approach of using worst case values is also quite heuristic in nature and doesn't guarantee that a design meets a desired probability of failure specification. Reliability based design optimization (RBDO) methods have emerged to solve such problems. Designs obtained using RBDO ensure that the probability of failure due to parameter uncertainties is below a desired level.

Conventionally, researchers have formulated RBDO as a nested optimization problem referred to as the double-loop method. This formulation is computationally expensive because of the two levels of optimization required. The upper level optimization solves the standard design problem, while for each function call a number of reliability analysis are performed; these are the inner optimization problems. Solving such nested optimization problems can be cost prohibitive, especially for large scale high fidelity multidisciplinary systems. Moreover, the computational cost associated with RBDO grows exponentially as the number of random variables and the number of critical failure modes increase. To alleviate the high computational cost, researchers have developed sequential RBDO methods. However, such techniques typically lead to premature convergence and, hence, yield spurious optimal designs. In the research by Agarwal *et al.*,^{1,2} a new unilevel formulation for performing RBDO was developed. The formulation provided for improved robustness and provable convergence as compared to a unilevel variant given by Kuschel and Rackwitz.³ In this new unilevel approach, the basic idea is to replace the *inverse* first order reliability method (FORM) by its first order Karush-Kuhn-Tucker (KKT) necessary optimality conditions at the upper level optimization. This unilevel method was shown to be computationally equivalent to the original nested optimization problem if the lower level optimization problem is solved by satisfying the KKT necessary condition.

RBDO, in general, is still relatively expensive when compared to deterministic optimization that doesn't account for design uncertainty. This expense has put limits on the types of problem to which it can be applied. For instance, high fidelity simulation models which require considerable computational cost may not be able to converge under design cycle time constraints. Attempts at reducing this cost have used approximation models such as kriging⁴ and correction response surfaces.⁵ These methods, however, don't converge to the true optimal solution of the high fidelity system. In this research, variable fidelity methods are used in conjunction with the double-loop method to reduce the computational cost of obtaining a reliable design, while guaranteeing convergence to the high fidelity solution, provided a suite of fidelity models are available. Variable fidelity methods have recently become more efficient and provide a framework for using lower fidelity models to reduce computational cost.⁶⁻¹⁰ The basic concept in these methods is to reduce the number of high fidelity function calls by using lower fidelity models and scaling functions that update the low fidelity model to match the higher fidelity result. The bulk of the computational time is used for evaluating the low fidelity model, while using limited high fidelity calls to ensure the scaling function is accurate.

In this paper an overview of RBDO is given along with brief details of the double-loop method, followed by a description of the variable fidelity framework. Next the combined variable fidelity reliability based design optimization (VF-RBDO) approach is detailed. This approach is then applied to two design problems to demonstrate the computational savings. The problems include an analytic test problem and a higher-dimensional high-lift airfoil design problem.

II. Deterministic Design Optimization

In solving a deterministic design optimization problem, the designer seeks the optimum values of design variables for which a merit function is the minimum and the deterministic constraints are satisfied. A standard form of the deterministic design optimization problem is:

$$\underset{\mathbf{x}}{\text{minimize}} \quad f(\mathbf{x}, \mathbf{p}) \quad (1)$$

$$\text{subject to} \quad g_i^R(\mathbf{x}, \mathbf{p}) \geq 0, \quad i = 1, \dots, N_R, \quad (2)$$

$$g_j^D(\mathbf{x}, \mathbf{p}) \geq 0, \quad j = 1, \dots, N_D, \quad (3)$$

$$\mathbf{x}^l \leq \mathbf{x} \leq \mathbf{x}^u, \quad (4)$$

where \mathbf{x} are the design variables and \mathbf{p} are the fixed parameters of the optimization problem. g_i^R is the i^{th} hard constraint that models the i^{th} critical failure mechanism of the system (e.g., stress, deflection, loads, etc). g_j^D is the j^{th} deterministic constraint due to other design considerations that are not affected by parameters or variables that could be uncertain. The design space is bounded by \mathbf{x}^l and \mathbf{x}^u . The merit function and the constraints are explicit functions of \mathbf{x} and \mathbf{p} .

A deterministic optimization formulation does not account for the uncertainties in the design variables and parameters. Optimized designs based on a deterministic formulation are usually associated with a high probability of failure because of the likely violation of certain hard constraints. This is particularly true if the hard constraints are active at the deterministic optimum solution. In today's competitive marketplace, it is very important that the resulting designs are optimal as well as reliable. This is usually achieved by replacing a deterministic optimization formulation with a *reliability based design optimization* formulation, where the critical hard constraints are replaced with reliability constraints.

III. Reliability Based Design Optimization

In the last two decades, researchers have proposed a variety of frameworks for efficiently performing reliability based design optimization. A survey of the literature reveals that the various RBDO methods can be divided into two broad categories: double-loop methods and sequential methods. Both of these approaches

make use of a reliability analysis technique to determine how reliable a given design is. These methods are explained in the following sections.

Reliability based design methods tend to move optimal designs away from failure driven constraints so that the uncertainties lead to a much lower chance of failure. This concept is shown pictorially in Figure 1. In the figure, point A is a deterministic design that is located on a failure driven constraint. When uncertainty is considered this single design point is replaced by a probability distribution of designs produced using the design parameters of point A. This figure shows that a good deal of this distribution about point A is in the failure domain. Point B with its respective probability distribution has a much lower chance of producing designs that fail. RBDO locates designs, like point B, that have a given measure of reliability while also trying to optimize an objective or cost function. In other words, RBDO methods attain the target reliably while minimizing the tradeoff from the objective.

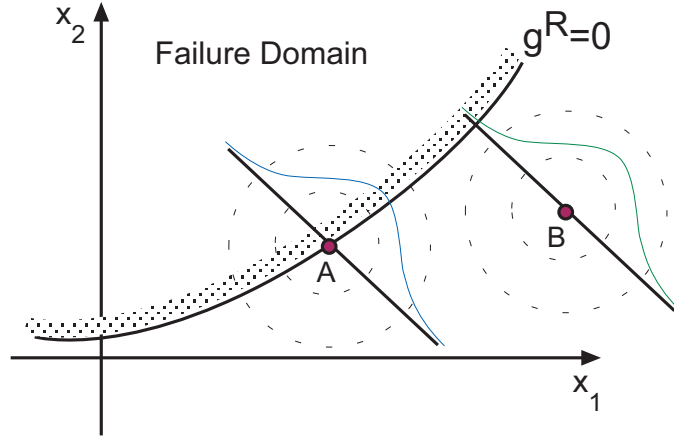


Figure 1. Reliability based optimization produce designs away from failure driven constraints.

A. Double Loop Methods for RBDO

Traditionally, the reliability based optimization problem has been formulated as a double loop optimization problem. In a typical RBDO formulation, the critical hard constraints from the deterministic formulation are replaced by reliability constraints, as in

$$\underset{\mathbf{x}}{\text{minimize}} \quad f(\mathbf{x}, \mathbf{p}) \quad (5)$$

$$\text{subject to} \quad \mathbf{g}^{rc}(\mathbf{V}, \boldsymbol{\eta}) \geq 0, \quad (6)$$

$$g_j^D(\mathbf{x}, \mathbf{p}) \geq 0, \quad j = 1, \dots, N_D, \quad (7)$$

$$\mathbf{x}^l \leq \mathbf{x} \leq \mathbf{x}^u, \quad (8)$$

where \mathbf{g}^{rc} are the reliability constraints. They are either constraints on probabilities of failure corresponding to each hard constraint or are a single constraint on the overall system's probability of failure. In this paper, only component failure modes are considered. It should be noted that the reliability constraints depend on the random variables \mathbf{V} and limit state parameters $\boldsymbol{\eta}$. The distribution parameters of the random variables are obtained from the design variables \mathbf{x} and the fixed parameters \mathbf{p} . (See the section on reliability analysis below.) \mathbf{g}^{rc} can be formulated as

$$g_i^{rc} = P_{t_i} - P_i, \quad i = 1, \dots, N_R, \quad (9)$$

where P_i is the failure probability of the hard constraint g_i^R at a given design, and P_{t_i} is the target allowable probability of failure for this failure mode. The probability of failure is usually estimated by employing

standard reliability techniques. A brief description of standard reliability methods is given in the next section. It has to be noted that the RBDO formulation given above (Equations (5)-(8)) assumes that the violation of soft constraints due to variational uncertainties is permissible and can be traded off for more reliable designs. For practical problems, design robustness represented by the merit function, and the soft constraints could be a significant issue, one that would require the solution to a hybrid robustness and reliability based design optimization formulation.

1. Reliability Analysis

Reliability analysis is a tool to compute the reliability index or the probability of failure corresponding to a given failure mode or for the entire system.¹¹ The uncertainties are modeled as continuous random variables, $\mathbf{V} = (V_1, V_2, \dots, V_n)^T$, with a known (or assumed) joint cumulative distribution function (CDF), $F_{\mathbf{V}}(\mathbf{v})$. The design variables, \mathbf{x} , consist of either distribution parameters $\boldsymbol{\theta}$ of the random variables \mathbf{V} , such as means, modes, standard deviations, and coefficients of variation, or deterministic parameters, also called limit state parameters, denoted by $\boldsymbol{\eta}$. The design parameters \mathbf{p} consist of either the means, the modes, or any first order distribution quantities of certain random variables. Mathematically this can be represented by the statements:

$$[\mathbf{p}, \mathbf{x}] = [\boldsymbol{\theta}, \boldsymbol{\eta}], \quad (10)$$

$$\mathbf{p} \text{ is a subvector of } \boldsymbol{\theta}. \quad (11)$$

Random variables can be consistently denoted as $\mathbf{V}(\boldsymbol{\theta})$, and the i^{th} failure mode can be denoted as $g_i^R(\mathbf{V}, \boldsymbol{\eta})$. In the following, \mathbf{v} denotes a realization of the random variables \mathbf{V} , and the subscript i is dropped without loss of clarity. Letting $g^R(\mathbf{v}, \boldsymbol{\eta}) \leq 0$ represent the failure domain, and $g^R(\mathbf{v}, \boldsymbol{\eta}) = 0$ be the so-called limit state function, the time-invariant probability of failure for the hard constraint is given by

$$P(\boldsymbol{\theta}, \boldsymbol{\eta}) = \int_{g^R(\mathbf{v}, \boldsymbol{\eta}) \leq 0} f_{\mathbf{V}}(\mathbf{v}) \, d\mathbf{v}, \quad (12)$$

where $f_{\mathbf{V}}(\mathbf{v})$ is the joint probability density function (PDF) of \mathbf{V} . It is usually impossible to find an analytical expression for the above integral. In standard reliability techniques, a probability distribution transformation $T: \mathbb{R}^n \rightarrow \mathbb{R}^n$ is usually employed. An arbitrary n -dimensional random vector $\mathbf{V} = (V_1, V_2, \dots, V_n)^T$ is mapped into an independent standard normal vector $\mathbf{U} = (U_1, U_2, \dots, U_n)^T$. This transformation is known as the *Rosenblatt Transformation*.¹² This transformation is depicted in Figure 2. The standard normal random variables are characterized by a zero mean and unit variance. The limit state function in \mathbf{U} -space can be obtained as $g^R(\mathbf{v}, \boldsymbol{\eta}) = g^R(T^{-1}(\mathbf{u}), \boldsymbol{\eta}) = G^R(\mathbf{u}, \boldsymbol{\eta}) = 0$. The failure domain in \mathbf{U} -space is $G^R(\mathbf{u}, \boldsymbol{\eta}) \leq 0$. Equation (12) thus transforms to

$$P_i(\boldsymbol{\theta}, \boldsymbol{\eta}) = \int_{G^R(\mathbf{u}, \boldsymbol{\eta}) \leq 0} \phi_{\mathbf{U}}(\mathbf{u}) \, d\mathbf{u}, \quad (13)$$

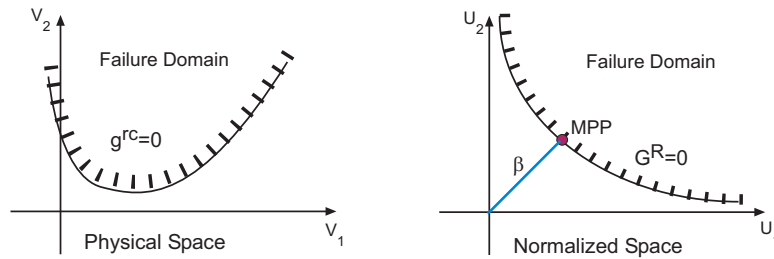


Figure 2. Transformation of the failure domain to a normalized space makes it possible to locate the MPP.

where $\phi_{\mathbf{U}}(\mathbf{u})$ is the standard normal density. If the limit state function in \mathbf{U} -space is affine, i.e., if $G^R(\mathbf{u}, \boldsymbol{\eta}) = \boldsymbol{\alpha}^T \mathbf{u} + \beta$, then an exact result for the probability of failure is $P_f = \Phi(-\frac{\beta}{\|\boldsymbol{\alpha}\|})$, where $\Phi(\cdot)$ is the cumulative Gaussian distribution function. If the limit state function is close to being affine, i.e., if $G^R(\mathbf{u}, \boldsymbol{\eta}) \approx \boldsymbol{\alpha}^T \mathbf{u} + \beta$ with $\beta = -\boldsymbol{\alpha}^T \mathbf{u}^*$, where \mathbf{u}^* is the solution of the following optimization problem,

$$\min \quad \|\mathbf{u}\| \quad (14)$$

$$\text{subject to} \quad G^R(\mathbf{u}, \boldsymbol{\eta}) = 0, \quad (15)$$

then the first order estimate of the probability of failure is $P_f = \Phi(-\frac{\beta}{\|\boldsymbol{\alpha}\|})$, where $\boldsymbol{\alpha}$ represents a normal to the manifold (15) at the solution point. The solution \mathbf{u}^* of the above optimization problem, the so-called design point, β -point or the *most probable point* (MPP) of failure, defines the reliability index $\beta_p = -\frac{\boldsymbol{\alpha}^T \mathbf{u}^*}{\|\boldsymbol{\alpha}\|}$. This method of estimating the probability of failure is known as the first order reliability method (FORM).¹¹

In the second order reliability method (SORM), the limit state function is approximated as a quadratic surface. A simple closed form solution for the probability computation using a second order approximation was given by Breitung¹³ using the theory of asymptotic approximations as

$$\begin{aligned} P_f(\boldsymbol{\theta}, \boldsymbol{\eta}) &= \int_{G^R(\mathbf{u}, \boldsymbol{\eta}) \leq 0} \phi_{\mathbf{U}}(\mathbf{u}) \, d\mathbf{u} \\ &\approx \Phi(-\beta_p) \prod_{l=1}^{n-1} (1 - \kappa_l)^{-1/2}, \end{aligned} \quad (16)$$

where κ_l is related to the principal curvatures of the limit state function at the minimum distance point \mathbf{u}^* , and β_p is the reliability index using FORM. Breitung¹³ showed that the second-order probability estimate asymptotically approaches the first order estimate as β_p approaches infinity, if $\beta_p \kappa_l$ remains constant.

The first order approximation, $P_f \approx \Phi(-\beta_p)$, is sufficiently accurate for most practical cases. Thus, only first order approximations of the probability of failure are used in practice. Using the FORM estimate, the reliability constraints in Equation (9) can be written in terms of reliability indices as

$$g_i^{rc} = \beta_i - \beta_{t_i}, \quad (17)$$

where β_i is the first order reliability index, and $\beta_{t_i} = -\Phi^{-1}(P_{allow_i})$ is the desired reliability index for the i^{th} hard constraint. When the reliability constraints are formulated as given in Equation (17), the approach is referred to as the *reliability index approach* (RIA).

It should be noted that the reliability analysis involves a probability distribution transformation, the search for the MPP, and the evaluation of the cumulative Gaussian distribution function. To solve the FORM problem (Equations 14-15), various algorithms have been reported in the literature.¹⁴ The solution typically requires many system analysis evaluations. Moreover, there might be cases where the optimizer may fail to provide a solution to the FORM problem, especially when the limit state surface is far from the origin in \mathbf{U} -space or when the case $G^R(\mathbf{u}, \boldsymbol{\eta}) = 0$ never occurs at a particular design variable setting.

In design automation it is not known *a priori* what design points the upper level optimizer will visit; therefore, it is not known if the optimizer for the FORM problem will provide a consistent result. This problem was addressed recently by Padmanabhan and Batill¹⁵ by using a trust region algorithm for equality constrained problems. For cases when $G^R(\mathbf{u}, \boldsymbol{\eta}) = 0$ does not occur, the algorithm provided the best possible solution for the problem through

$$\min \quad \|\mathbf{u}\| \quad (18)$$

$$\text{subject to} \quad G^R(\mathbf{u}, \boldsymbol{\eta}) = c. \quad (19)$$

The reliability constraints formulated by the RIA are, therefore, not robust. RIA is usually more effective if the probabilistic constraint is violated, but it yields a singularity if the design has zero failure probability.¹⁶ To overcome this difficulty, Tu *et al.*¹⁶ provided an improved formulation to solve the RBDO problem. In this method, known as the *performance measure approach* (PMA), the reliability constraints are stated by an inverse formulation as

$$g_i^{rc} = G_i^R(\mathbf{u}_{\beta=\beta_i}^*, \boldsymbol{\eta}) \quad i = 1, \dots, N_R. \quad (20)$$

\mathbf{u}_i^* is the solution to the inverse reliability analysis (IRA) optimization problem

$$\min \quad G_i^R(\mathbf{u}, \boldsymbol{\eta}) \quad (21)$$

$$\text{subject to} \quad \|\mathbf{u}\| = \beta_{t_i}, \quad (22)$$

where the optimum solution $\mathbf{u}_{\beta=\beta_i}^*$ corresponds to MPP in IRA of the i^{th} hard constraint. Solving RBDO by the PMA formulation is usually more efficient and robust than the RIA formulation where the reliability is evaluated directly. The efficiency lies in the fact that the search for the MPP of an inverse reliability problem is easier to solve than the search for the MPP corresponding to an actual reliability. The RIA and the PMA approaches for RBDO are essentially inverse of one another and would yield the same solution if the constraints are active at the optimum.¹⁶ If the constraint on the reliability index (as in the RIA formulation) or the constraint on the optimum value of the limit-state function (as in the PMA formulation) is not active at the solution, the reliable solution obtained from the two approaches might differ.

Similar RBDO formulations were independently developed by other researchers.^{17–19} In these RBDO formulations, constraint (22) is considered as an inequality constraint ($\|\mathbf{u}\| \leq \beta_{t_i}$), which is a more robust way of handling the constraint on the reliability index. The major difference lies in the fact that in these papers' semi-infinite optimization algorithms were employed to solve the RBDO problem. Semi-infinite optimization algorithms solve the inner optimization problem approximately. However, the overall RBDO is still a nested double-loop optimization procedure. As mentioned earlier, such formulations are computationally intensive for problems where the function evaluations are expensive. Moreover, the formulation becomes impractical when the number of hard constraints increase, which is often the case in real-life design problems. To alleviate the computational cost associated with the nested formulation, sequential RBDO methods have been developed.

B. Sequential Methods for RBDO

Sequential RBDO methods include a variety of different approaches proposed by different researchers. Chen and Du²⁰ developed a decoupled sequential probabilistic design methodology. In this framework, the deterministic optimization and the reliability assessment are decoupled from one another. During each cycle, a deterministic optimization problem is solved, followed by reliability assessment and a convergence check. Chen *et al.*²¹ also developed a sequential RBDO methodology that was recently generalized for non-normal distributions by Wang and Kodiyalam²² and extended for multidisciplinary systems by Agarwal *et al.*²³ In this methodology, the lower-level optimization is eliminated, and the MPP of failure corresponding to the probabilistic constraints is estimated implicitly by using a nonlinear transformation based on the direction cosines of the hard constraints at the mean values of the random variables. This methodology is shown to be extremely efficient. However, for highly nonlinear limit state functions, the estimate of the MPP of failure given by the nonlinear transformation might be very different from the actual MPP of failure, and the framework may fail to converge to the true solution. The drawback of sequential RBDO methodologies is that a local optimum cannot be guaranteed. Such methodologies can lead to spurious optimal designs.

It has been noted that the traditional reliability based optimization problem is a nested optimization problem. Solving such nested optimization problems for a large number of failure driven constraints and/or nondeterministic variables is extremely expensive. Researchers have developed sequential approaches to speed up the optimization process and to obtain a consistent reliability based design. To address the issue of obtaining spurious optimal designs, a new sequential optimization strategy for reliability based design is developed in Agarwal *et al.*²⁴

At this point the ground work for doing RBDO has been described. The RBDO methods inherently have a much higher computational cost than doing deterministic optimization. In order to make RBDO computationally trackable for expensive problems, variable fidelity optimization methods are employed in this investigation to reduce the computational cost. The ability to use such methods assumes that a suite of fidelity models can be provided. In the next section variable fidelity methods are discussed.

IV. Variable Fidelity Optimization

The typical framework for variable fidelity optimization is depicted in Figure 3 and is based, in part, on work done by Alexandrov²⁵ and is fully described by Gano *et al.*⁶ This framework is designed to reduce the number of high fidelity function calls by using a scaling function and lower fidelity models. The following process describes the basic steps of the framework:

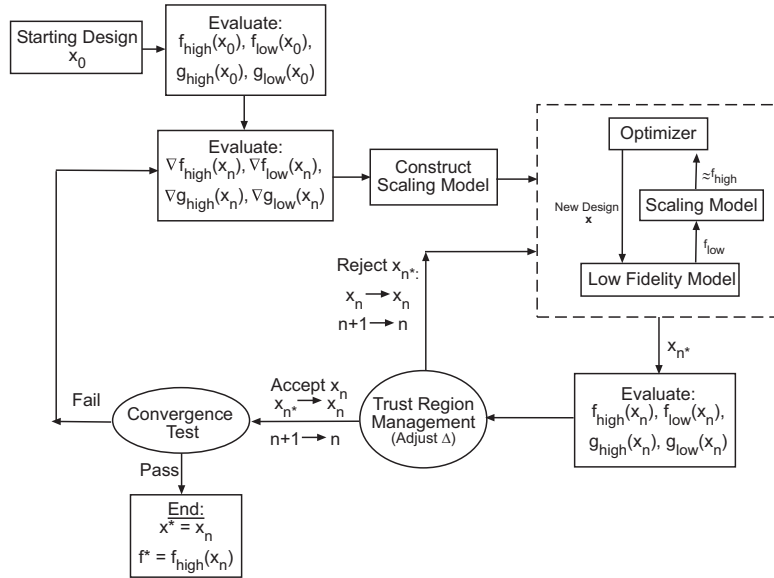


Figure 3. Variable fidelity framework flowchart.

Step 1 Initialization: The objective and constraints are evaluated using both the high and low fidelity models at the starting design point, \mathbf{x}_0 . Also an initial l_1 penalty function is evaluated (see Step 5).

Step 2 Gradient Evaluation: The gradient of the objective and the Jacobian for the constraints are evaluated using both the high and low fidelity models at the current design point, \mathbf{x}_n .

Step 3 Construct Scaling Model: A scaling model is constructed to insure matching between the fidelity models. This model can be based on many different methods; additive and multiplicative are the most common and are discussed in more detail later. Each method can be modeled as first order, second order, or kriging based. A scaling model is constructed for each constraint as well as for the objective function.

Step 4 Optimize Scaled Low Fidelity Model: The low fidelity model scaled with the scaling model constructed in Step 3 is optimized. The choice of optimizer used is based on preference. In the work done by Alexandrov,⁸ three optimizers were compared: augmented Lagrangian method, multilevel algorithms for large-scale constrained optimization (MAESTRO)²⁶ (used for coupled MDO problems), and sequential quadratic programming (SQP). For typical single discipline problems, Alexandrov found SQP to be the most promising, and it is used in this research. The unscaled constraints are included in this step to ensure that they are always satisfied.

Step 5 Evaluate New Design and l_1 Penalty Function: Using the resulting design point from Step

4, the high fidelity objective and constraints are evaluated. The objective and constraint values are used to calculate a current value of the l_1 penalty function, P , for the high and scaled low fidelity models. The penalty function is defined as

$$P(\mathbf{x}) = f(\mathbf{x}) + \frac{1}{\mu_n} \sum \max(0, g_i(\mathbf{x})) + \frac{1}{\mu_n} \sum |h_i(\mathbf{x})|, \quad (23)$$

where μ is the penalty weight which is typically decreased by a factor of ten each time a new point is accepted. This penalty weighting drives all the active constraints to zero as the algorithm converges.

Step 6 Trust Region Management: In order to guarantee convergence of the variable fidelity optimization framework, a trust region model management strategy is employed.²⁷ This method provides a means for adaptively managing the allowable move limits for the approximate design space. Originally these methods were used to ensure the convergence of Newton based methods.

A trust region ratio allows the trust region model management framework to monitor how well the approximation matches the high fidelity design space. After each completed optimization on the scaled low fidelity model, a new candidate point, \mathbf{x}_n^* , is found. A trust region ratio, ρ_n , is calculated at this new point:

$$\rho_n = \frac{P(\mathbf{x}_n)_{high} - P(\mathbf{x}_n^*)_{high}}{P(\mathbf{x}_n)_{scaled} - P(\mathbf{x}_n^*)_{scaled}}, \quad (24)$$

where $P()_{high}$ and $P()_{scaled}$ are the l_1 penalty functions for the high and scaled low fidelity models and the point \mathbf{x}_n was the initial point of the optimization. Notice that by definition $P(\mathbf{x}_n)_{scaled} = P(\mathbf{x}_n)_{high}$, because the scaled low fidelity model matches the high fidelity model at that point. This is the ratio of the actual change in the function to the predicted change of the function by the scaled lower fidelity model. Because the constraints are also approximated, the trust region ratio must account for this and converge to a feasible design. That is the reasoning behind using the l_1 penalty function.

The trust region size is governed by the following standard rules:^{28,29}

$$\Delta_{n+1} = \begin{cases} c_1 \Delta_n & : \rho_n \leq R_1 \vee \rho_n > R_3 \\ \Delta_n & : R_1 < \rho_n < R_2 \\ \Gamma \Delta_n & : R_2 \leq \rho_n \leq R_3 \end{cases} \quad (25)$$

where $\Gamma = c_2$ if $\|x_k^* - x_{c_k}\|_\infty = \Delta_k$ otherwise $\Gamma = 1$. A typical set of values for the range limiting constants are $R_1 = 0.25$, $R_2 = 0.75$, and $R_3 = 1.25$, while the trust region multiplication factors are typically $c_1 = 0.25$ and $c_2 = 3$. Physically, ρ represents how good of an approximation our scaled low fidelity model is compared to the high fidelity model. If ρ is near 1, the approximation is quite good. If ρ is near zero, the approximation is not as good, but still captures the minimization trend. If ρ is negative, then the point is a worse design. In this case the point is rejected, the trust region size is reduced by the factor c_1 , and the algorithm returns to Step 4. As long as $\rho > 0$, the point is accepted and the algorithm proceeds to Step 7.

Step 7 Convergence Test: The convergence of the entire framework is governed by satisfying the Karush-Kuhn-Tucker conditions as is done by Rodríguez *et al.*³⁰ and Conn *et al.*³¹ For the implementation used in this research the convergence was determined by the following two inequalities:

$$f_{high}(\mathbf{x}_n) - f_{high}(\mathbf{x}_{n-1}) < \epsilon_f, \quad (26)$$

$$\|\mathbf{x}_n - \mathbf{x}_{n-1}\| < \epsilon_x, \quad (27)$$

where ϵ_f and ϵ_x are tolerances supplied by the user, and n is the current iteration counter. If any of the two inequalities at the current point is true, the algorithm is considered converged. If the convergence test is true, then the final design is found, otherwise, the algorithm returns to Step 2.

A. Scaling Methods

Existing variable fidelity or approximate model management frameworks come in two varieties: multiplicative or additive. Currently, the most common is the multiplicative framework, devised by Alexandrov and Lewis³² based on Chang's³³ scaling function. The additive method was presented by Lewis and Nash.³⁴ Both methods are based on constructing an unknown function to update the lower fidelity model, which in turn, will approximate the higher fidelity model.

1. Multiplicative Scaling

A given set of high and low fidelity models, $f_{high}(\mathbf{x})$ and $f_{low}(\mathbf{x})$, can be matched by multiplying the low fidelity model by an unknown function $\beta(\mathbf{x})$. This is posed mathematically as

$$f_{high}(\mathbf{x}) = \beta(\mathbf{x})f_{low}(\mathbf{x}). \quad (28)$$

This scaling model was first proposed and used for approximating structural response by Chang *et al.*³³ Solving for the unknown multiplicative scaling function results in

$$\beta(\mathbf{x}) = \frac{f_{high}(\mathbf{x})}{f_{low}(\mathbf{x})}. \quad (29)$$

From inspection of Equation 29, it is clear that the function $\beta(\mathbf{x})$ is the scaling ratio of the high fidelity model to the low fidelity model, and when it is multiplied by the low fidelity model, the response of the high fidelity model is achieved.

2. Additive Scaling

A given set of high and low fidelity models, $f_{high}(\mathbf{x})$ and $f_{low}(\mathbf{x})$, can also be matched by adding the low fidelity model to an unknown function $\gamma(\mathbf{x})$. This is expressed mathematically as

$$f_{high}(\mathbf{x}) = f_{low}(\mathbf{x}) + \gamma(\mathbf{x}). \quad (30)$$

The additive scaling function can be solved for, by subtracting the low fidelity function from both sides:

$$\gamma(\mathbf{x}) = f_{high}(\mathbf{x}) - f_{low}(\mathbf{x}). \quad (31)$$

From Equation 31, it is clear that the function $\gamma(\mathbf{x})$ is the additive scaling of the high fidelity model to the low fidelity model, or the error between them. When this function is added to the low fidelity model, the response of the high fidelity model is produced. A similar function for the constraints can be developed in the same manner as Equations (30) and (31).

3. Adaptive Hybrid Scaling - Combining Additive and Multiplicative Methods

In general, some suites of fidelity models are matched better using one method or the other or possibly some linear combination of the two models, and there is no way to know this *a priori*. This section describes a methodology that adaptively combines both types of scaling.

Combining both the multiplicative and additive scaling functions such that they still properly scale the low fidelity model to match the high fidelity model requires the use of a weighted average of the two methods. The weighted averaging maintains the Taylor series matching and, therefore, retains the convergence properties. Using a weighting term, \mathcal{W} , this sum is

$$f_{high}(\mathbf{x}) = \mathcal{W}f_{low}(\mathbf{x})\beta(\mathbf{x}) + (1 - \mathcal{W})(f_{low}(\mathbf{x}) + \gamma(\mathbf{x})). \quad (32)$$

To determine the value of \mathcal{W} , a further condition must be enforced.⁷ proposes to use a previously evaluated point to adjust the value of \mathcal{W} such that the model passes through that point as well. The weighting function then takes the value

$$\mathcal{W} = \frac{f_{high}(\mathbf{x}_{pp}) - (f_{low}(\mathbf{x}_{pp}) + \gamma(\mathbf{x}_{pp}))}{f_{low}(\mathbf{x}_{pp})\beta(\mathbf{x}_{pp}) - (f_{low}(\mathbf{x}_{pp}) + \gamma(\mathbf{x}_{pp}))}. \quad (33)$$

In Equation 33 the current additive and multiplicative scaling functions are used along with any previous point, \mathbf{x}_{pp} , where the high fidelity model was evaluated. There is some freedom in choosing the past point. One option is to simply use the last accepted design point. However, for this work the nearest point is used. The advantage of using the nearest point is that it could have been a design that was evaluated but rejected; this would help keep the next iteration from moving in this undesired direction. A new weighting value can be computed both for the objective and each constraint at each iteration. Updating these weights at each iteration allows the framework to *adapt* to the best model for the current area of the design space.

B. First Order Scaling Methods

The different scaling functions must be approximated. In this section the first order approximations are presented; a higher order method is presented in the next section. The first order multiplicative approximation model is found using Chang's³³ scaling function $\beta(\mathbf{x})$. At a given design point, for example the current design, this function is defined as

$$\beta(\mathbf{x}_n) = \frac{f_{high}(\mathbf{x}_n)}{f_{low}(\mathbf{x}_n)}. \quad (34)$$

This scaling factor at any other point can be approximated using a Taylor series to first order:

$$\tilde{\beta}(\mathbf{x}) = \beta(\mathbf{x}_n) + \nabla\beta(\mathbf{x}_n)^T(\mathbf{x} - \mathbf{x}_n). \quad (35)$$

To evaluate this, the gradient information is needed and can be obtained by differentiating Equation 34, resulting in

$$\nabla\beta(\mathbf{x}_n) = \begin{bmatrix} \frac{f_{low}(\mathbf{x}_n) \frac{\partial f_{high}}{\partial x_1} \Big|_{\mathbf{x}=\mathbf{x}_n} - f_{high}(\mathbf{x}_n) \frac{\partial f_{low}}{\partial x_1} \Big|_{\mathbf{x}=\mathbf{x}_n}}{f_{low}(\mathbf{x}_n)^2} \\ \vdots \\ \frac{f_{low}(\mathbf{x}_n) \frac{\partial f_{high}}{\partial x_m} \Big|_{\mathbf{x}=\mathbf{x}_n} - f_{high}(\mathbf{x}_n) \frac{\partial f_{low}}{\partial x_m} \Big|_{\mathbf{x}=\mathbf{x}_n}}{f_{low}(\mathbf{x}_n)^2} \end{bmatrix}, \quad (36)$$

Therefore, a first order update on the low fidelity model is

$$f_{high} \approx \tilde{\beta}(\mathbf{x})f_{low}. \quad (37)$$

This model insures that at the initial design point, the updated low fidelity model matches the function and the gradient of the high fidelity model. The identical process is done in order to scale each constraint.

The first order additive scaling method is similar to the first order multiplicative scaling method because it tries to approximate the high fidelity model by applying a correction to the lower fidelity model. The additive method was used by Lewis and Nash³⁴ to solve multigrid problems but can be used more generally.

At a given design point, the additive scaling function has the value

$$\gamma(\mathbf{x}_n) = f_{high}(\mathbf{x}_n) - f_{low}(\mathbf{x}_n). \quad (38)$$

This additive scaling factor at any other point can be approximated using a Taylor series to first order:

$$\tilde{\gamma}(\mathbf{x}) = \gamma(\mathbf{x}_n) + \nabla\gamma(\mathbf{x}_n)^T(\mathbf{x} - \mathbf{x}_n). \quad (39)$$

Evaluating this requires gradient information which can be obtained by differentiating Equation 38. This gives

$$\nabla\gamma(\mathbf{x}_n) = \nabla f_{high}(\mathbf{x}_n) - \nabla f_{low}(\mathbf{x}_n). \quad (40)$$

Therefore, a first order update on the low fidelity model is

$$f_{high}(\mathbf{x}) \approx f_{low}(\mathbf{x}) + \tilde{\gamma}(\mathbf{x}). \quad (41)$$

This model insures that at the current design point, the updated low fidelity model matches both the function and the gradient of the high fidelity model exactly, which is required for proof of convergence. Nearby points should also approximate the high fidelity response well.

C. Second Order Scaling Models

Using the same idea as in the first order method, an approximation scaling function can be derived to match second order information. This approach was first used by Gano *et al.*¹⁰ and Eldred *et al.*⁷ using both second order information and approximate second order information. The approach is analogous to the first order method except the Taylor series approximation is expanded to include the second order terms as the name implies. The result for the multiplicative method is

$$\tilde{\beta}(\mathbf{x}) = \beta(\mathbf{x}_n) + \Delta\mathbf{x}^T \nabla\beta(\mathbf{x}_n) + \frac{1}{2} \Delta\mathbf{x}^T \nabla^2\beta(\mathbf{x}_n) \Delta\mathbf{x}. \quad (42)$$

Using the same gradient result as in the first order method, the only remaining term needed is the Hessian of β ; this can be found by differentiating again, which simplifies to:

$$\nabla^2\beta(\mathbf{x}_n) = \begin{bmatrix} h_{1,1} & h_{1,2} & \cdots & h_{1,m} \\ h_{2,1} & \ddots & & \vdots \\ \vdots & & \ddots & \vdots \\ h_{m,1} & \cdots & \cdots & h_{m,m} \end{bmatrix}, \quad (43)$$

where

$$h_{i,j} = \frac{1}{f_{low}^3} \left(2f_{high} \frac{\partial f_{low}}{\partial x_i} \frac{\partial f_{low}}{\partial x_j} + f_{low}^2 \frac{\partial^2 f_{high}}{\partial x_i \partial x_j} - f_{low} \left(\frac{\partial f_{low}}{\partial x_j} \frac{\partial f_{high}}{\partial x_i} + \frac{\partial f_{high}}{\partial x_j} \frac{\partial f_{low}}{\partial x_i} + f_{high} \frac{\partial^2 f_{low}}{\partial x_i \partial x_j} \right) \right), \quad (44)$$

where all the functions and partial derivatives are evaluated at the point \mathbf{x}_n and i and j are the indices for the Hessian matrix which run from 1 to the number of design variables.

For the additive method, the second order expansion is

$$\tilde{\gamma}(\mathbf{x}) = \gamma(\mathbf{x}_n) + \Delta\mathbf{x}^T \nabla\gamma(\mathbf{x}_n) + \frac{1}{2} \Delta\mathbf{x}^T \nabla^2\gamma(\mathbf{x}_n) \Delta\mathbf{x}. \quad (45)$$

The first order information was derived in the previous section. Again, the only remaining information needed is the Hessian of γ ; this can be found by taking the gradient of the gradient of γ :

$$\nabla^2\gamma(\mathbf{x}_n) = \nabla^2 f_{high}(\mathbf{x}_n) - \nabla^2 f_{low}(\mathbf{x}_n). \quad (46)$$

The scaling functions have the same form as those in the first order methods and can similarly be computed for the constraints as well as the objective function. Computing the symmetric full rank Hessian matrices of either of the second order methods would be quite expensive, even if gradient information was readily available.

1. Approximate Second Order Scaling

The second order information that is needed in both second order techniques can be very costly to compute. There exist techniques to approximate the second order information from first order information, which is calculated at each iteration of the variable fidelity optimization process. In this investigation the second order information can, therefore, be obtained at no additional cost, in terms of function calls, compared to the first order scaling methods. The two most prevalent methods used are the Broyden-Fletcher-Goldfarb-Shanno³⁵⁻³⁸ (BFGS) update and the symmetric-rank-1 (SR1) update.

V. Reliability Based Design Using Variable Fidelity Optimization

This section describes how the variable fidelity framework is used to reduce the computational expense of high fidelity reliability based design. This combined method will be henceforth referred to as variable fidelity reliability based design optimization (VF-RBDO).

Combining these two methods is a straightforward process; though, combining the two methods is a novel approach to lower the cost of RBDO. The variable fidelity framework is setup to do deterministic opposed to reliability optimization, which differ mainly in their formulation. In the reliability case the upper level constraints, which insure a specific level of reliability is attained, involve a sub-optimization process of finding the MPP for each of the deterministic constraints. The objective function is not typically altered, unless a robust design formulation is desired. Therefore, the objective function and the upper level constraints can be included into the variable fidelity framework directly as long as there exist at least two levels of fidelity models used in computing the system responses. A diagram for combining these two methods is given in Figure 4.

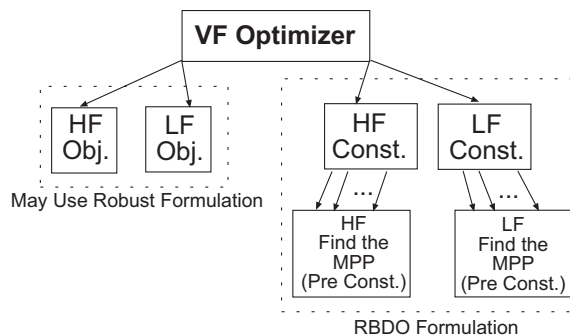


Figure 4. VF-RBDO framework

Another emerging RBDO method is to remove the the sub-optimization problems of finding the MPP for each constraint by instead including their first order Karush Kuhn Tucker conditions at the top level. By removing the nested optimization calls these methods have been shown to reduce the computational expense of RBDO.^{1,2} However, these methods increase the number of design variables significantly while also making the design space itself much more complicated by including many equality constraints. This complication may be augmented by using constraint relaxation methods such as homotopy³⁹ or by using approximations to solve the infeasible trust region problem.⁴⁰ Furthermore, unilevel methods require second order information which can be approximated. Because second order information is typically not available, using approximate second order information may hinder the convergence properties of the variable fidelity method. Combining the unilevel RBDO methods and the variable fidelity method would follow the same procedure as described above.

VI. Numerical Implementation Studies

To demonstrate the savings of using the VF-RBDO method it was applied to two problems. The first problem is a specific analytic problem referred to as the Barnes Problem. This problem will provide verification of the method and is two-dimensional for easier solution visualization. The second problem is an airfoil shape optimization problem that is subject to an uncertain Mach number and angle of attack. This problem is similar to problems used by Padula *et al.*^{41–43} for robust design. To compute the aerodynamic forces on the airfoils, various fidelity computational fluid dynamics (CFD) simulations are used.

A. Analytic Two Dimensional Problem

In order to help visualize the VF-RBDO methodology an analytic two-dimensional problem is solved first. The problem is known as the Barnes problem as it was originally formulated in his master’s thesis.⁴⁴ It is a highly nonlinear problem which makes it a challenge to solve, even though it has only two design variables. The original formulation of the problem was deterministic. Agarwal and Renaud⁴⁵ recast the problem as a reliability problem and renamed this formulation the Modified Barnes Problem. This modified version is used as the high fidelity model in this research. The problem has four random variables, \mathbf{V} , which are statistically independent and normally distributed. The means and standard deviations for these random variables are given in the problem formulation below. Two of the three constraints for this problem are failure driven, \mathbf{g}^R . The remaining constraint, g^D , is deterministic. The optimization problem is posed as follows.

$$\begin{aligned}
 &\underset{x_1, x_2}{\text{minimize}} && f(\mathbf{x}) = a_1 + a_2x_1 + a_3x_2^2 + a_4x_1^3 + a_5x_1^4 + a_6x_2 + a_7x_1x_2 + a_8x_1^2x_2 + a_9x_1^2x_2 \\
 & && + a_{10}x_1^4x_2 + a_{11}x_2^2 + a_{12}x_2^3 + a_{13}x_2^4 + \frac{a_{14}}{x_1+1} + a_{15}x_1^2x_2^2 + a_{16}x_1^3x_2^2 + a_{17}x_1^3x_2^3 \\
 & && + a_{18}x_1x_2^2 + a_{19}x_2x_2^3 + a_{20}e^{a_{21}x_1x_2} \\
 &\text{subject to:} && g_1^R = \frac{x_1x_2}{v_1} - v_2 \geq 0 \\
 & && g_2^R = \frac{x_2}{v_3} + \frac{x_1^2}{v_4} \geq 0 \\
 & && g^D = \left(\frac{x_2}{50} - 1\right)^2 - \left(\frac{x_1}{500} - 0.11\right) \geq 0 \\
 &\text{and} && 0 \leq x_1 \leq 75 \\
 & && 0 \leq x_2 \leq 65 \\
 &\text{where} && v_1 = N(700, 1), v_2 = N(1, 0.3), v_3 = N(5, 1), v_4 = N(25, 0.3)
 \end{aligned}$$

The coefficients of the objective function are given in Table 1. The RBDO formulation for this problem is

$$\begin{aligned}
 &\underset{x_1, x_2}{\text{minimize}} && f(\mathbf{x}) \\
 &\text{subject to:} && g_i^{rc} = \beta_i - 3 \geq 0, i = 1, 2 \\
 & && g^D \geq 0 \\
 &\text{and} && 0 \leq x_1 \leq 75 \\
 & && 0 \leq x_2 \leq 65 .
 \end{aligned}$$

Table 1. Coefficients for the Barnes problem.

a_1	7.5196E1	a_2	-3.8112E0	a_3	1.2694E-1	a_4	-2.0567E-3	a_5	1.0345E-5
a_6	-6.8306E0	a_7	3.0234E-2	a_8	-1.28134E-3	a_9	3.5256E-5	a_{10}	-2.2667E-7
a_{11}	2.5645E-1	a_{12}	-3.4604E-3	a_{13}	1.3514E-5	a_{14}	-2.8106E1	a_{15}	-5.2375E-6
a_{16}	-6.3000E-8	a_{17}	7.0000E-10	a_{18}	3.4054E-4	a_{19}	-1.6638E-6	a_{20}	-2.8673E0
a_{21}	5.0000E-4								

A low fidelity version of this problem is created by making a few changes to the problem which significantly alter the design space. In the objective function two coefficients, a_5 and a_{21} , are set to zero, reducing the

nonlinearity of the model. Also the first two constraints are altered, including a change of three mean values of the random variables. These modifications are summarized below.

$$a_{5low} = 0, a_{21low} = 0$$

$$g_{1low}^R = \frac{x_1 x_2}{v_{1low}} - v_{2low} \geq 0, g_{2low}^R = \frac{x_2}{v_3} + \frac{x_1}{v_{4low}^2} \geq 0$$

$$v_{1low} = N(750, 1), v_{2low} = N(0.5, 0.3), v_{4low} = N(4, 0.3)$$

Figure 5 shows the design spaces for both the high and low fidelity models. The high fidelity constraints are also shown in the low fidelity model for easier comparison. The high fidelity model has four local minima while the low fidelity model has only two; these points are represented in the figure by circles. The objective function contours of the two models have significant differences in value and in orientation. One would hope that in practice the low fidelity model would be a better match; however, this demonstration problem shows the robustness of the variable fidelity methodology.

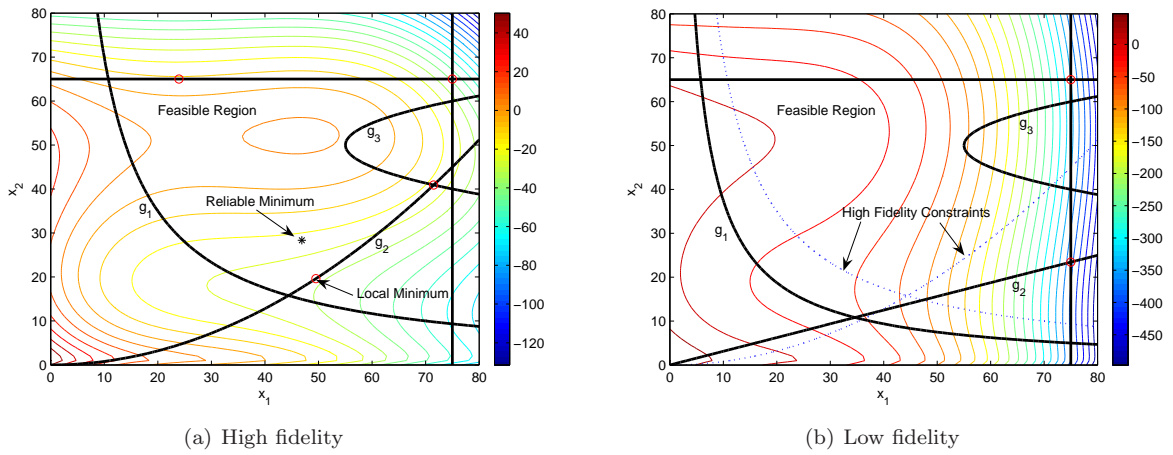


Figure 5. High and low fidelity design spaces of the Barnes Problem.

In both implementation studies, different variable fidelity scalings and models are compared for use in reliability based design optimization. These results are also compared using a standard sequential quadratic programming (SQP) method to solve the RBDO problem. MATLAB's *fmincon*⁴⁶ was used as the SQP solver. The different variable fidelity scaling methods used were the multiplicative, additive, and adaptive hybrid. Furthermore, for each scaling the first order and quasi-second order methods using BFGS and SR1 were compared. All of the trials were started at the point $\mathbf{x} = [40, 30]^T$ with an initial trust region size of $\Delta_0 = 10$. The results are summarized in Table 2.

All of the methods compared in Table 2 converged to the same solution. The objective of using these methods was to reduce the number of high fidelity function calls. Comparing the high fidelity function calls required for convergence between the standard SQP RBDO method and all of the VF-RBDO methods shows a significant savings. The 1st order multiplicative method performed the worst in this case; though, it still used 26% fewer high fidelity calls. The highest savings was obtained using the 2nd order additive method using the SR1 update to approximate the Hessian information, and it achieved a 71% reduction in high fidelity calls. All of the second order methods out-performed the first order methods. The adaptive hybrid method seemed to select the better of the two methods but didn't perform better than either one. One other factor that should be noticed when comparing these methods is that there was a much larger number of low fidelity function calls for the multiplicative method and the second order hybrid method. This could play a important factor, depending on the relative costs between the suite of fidelity models, so it is further studied in the next problem.

Table 2. VF-RBDO double-loop PMA results for the modified Barnes problem.

Method	HF Fn Evals	LF Fn Evals	Iters
Multiplicative Scaling			
1st Order	952	5580	12
2nd Order, BFGS	489	9571	7
2nd Order, SR1	442	5465	6
Additive Scaling			
1st Order	440	4439	7
2nd Order, BFGS	405	3001	6
2nd Order, SR1	377	3001	6
Adaptive Hybrid Scaling			
1st Order	481	3981	7
2nd Order, BFGS	409	6477	6
2nd Order, SR1	390	6590	6
RBDO SQP	1295	-	9

B. Energy Efficient Transport High-Lift Airfoil Design

For about two decades, starting in the mid 1970s, the National Aeronautics and Space Administration (NASA) conducted research to improve the efficiency of jet transport aircraft. Part of this research effort included the energy efficient transport program, which developed supercritical airfoils with larger section thickness-to-chord ratios, higher aspect ratios, higher cruise lift coefficients, and less swept wings. Because these wings had higher lift at cruise they could be smaller and more fuel efficient. With the reduced wing area, these new wings needed a high-lift flap system to ensure that takeoff and landing requirements could be met.

The problem solved here is: given a high-lift airfoil, find the optimal placement of its slat, vane, and flap to provide maximum lift for takeoff or landing configurations. The problem was developed from the experimental and numerical work done at NASA Langley.⁴⁷⁻⁴⁹ The problem consists of nine design variables which control the horizontal, vertical, and rotational orientation of the slat vane and flap relative to their cruise configuration. The rotation is measured positive counter-clockwise about each control surface's leading edge. Figure 6 shows the layout of the multi-element supercritical airfoil in both cruise and high-lift configurations. Figure 6 also shows the three degrees of freedom the control surfaces can move. Two failure driven constraints were placed on the lift to drag ratio and on the moment produced by the airfoil configuration. A deterministic constraint was placed on the distance, or gap, between the elements for gridding purposes. The deterministic design problem is formulated below.

$$\begin{aligned}
 & \underset{\mathbf{x}}{\text{maximize}} && c_l \\
 & \text{subject to:} && \frac{c_l}{c_d} \geq 85 \\
 & && c_m \leq 0.65 \\
 & && \text{gaps} \geq 1 \times 10^{-6}
 \end{aligned}$$

The flow conditions for the problem consisted of a Reynolds number of 9 million, a Mach number of 0.3, and an angle of attack 3 degrees. For the RBDO problem formulations the Mach number and angle of attack were considered as random variables. The lift, drag, and moment coefficients are all functions of the 9 design variables and of the Mach number and angle of attack. The deterministic values of Mach number and angle of attack are taken to be their mean values with both being normally distributed with variances of 5% of their respective mean values.

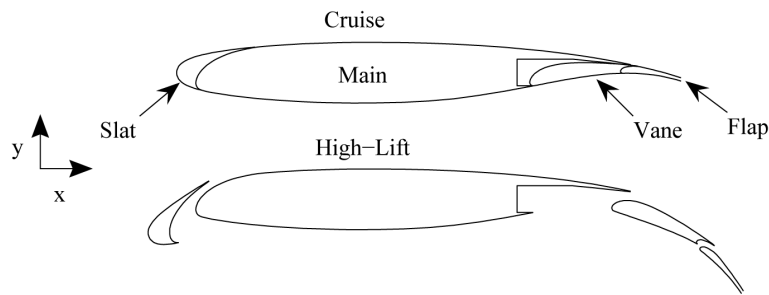
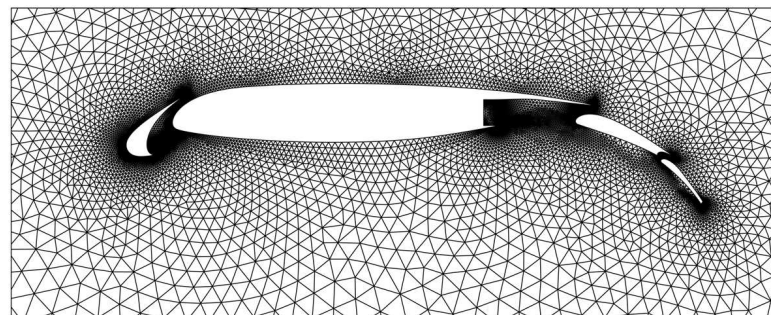
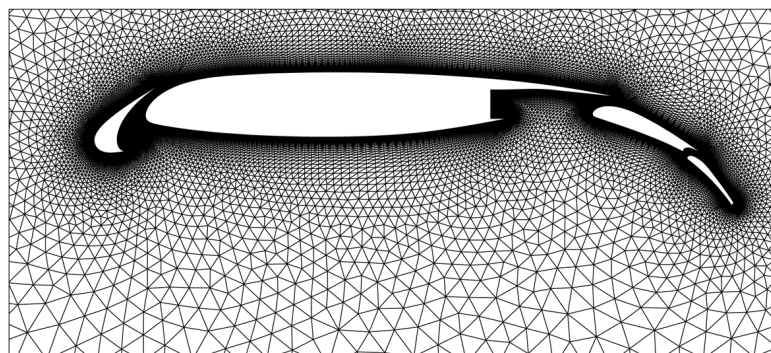


Figure 6. Cruise and high-lift configurations for EET airfoil.

The flow was solved using the inviscid Euler's equations for the low fidelity model. The grid consisted of about 45,000 elements, as seen in Figure 7a, which extended to 30 times the chord length in each direction. For the high fidelity model, a full Navier-Stokes solution was used; the grid consisted of about 100,000 elements as seen in Figure 7b. The CFD runs took approximately 9 minutes and 2.5 hours for the low and high fidelity models respectively. To further reduce the computation expense of the low fidelity model, a kriging-surrogate was created, reducing the expense to approximately a second. It should also be noted that a surrogate was created and used for the high fidelity model for the purpose of reducing the cost to a tractable level for demonstration purposes, which follows from the work done by Alexandrov.⁸



(a) Low fidelity - inviscid, approximately 45,000 elements



(b) High fidelity - viscid, approximately 100,000 elements

Figure 7. Close up view of the high and low fidelity unstructured CFD grids used in the AEEET problem.

Both fidelity models were solved using a computational fluid dynamics package developed at NASA Langley called FUN2D.^{50,51} This package uses fully unstructured mesh, which was generated using the advancing-front local-reconnection method described by Marcum.^{52,53}

In comparing the various VF-RBDO methods the main goal is to reduce the number of high fidelity function calls and ultimately the total time needed to find an optimal design. For each case the total of high and low fidelity function calls were tallied along with an estimate of computational expense required. This computational expense, or relative cost, was calculated using a weight of 2.5 time units for a high fidelity function call and 0.15 units per low fidelity function call. The precise computational expense couldn't be determined because of the use of the kriging models in place of the true CFD models. The results from the VF-RBDO double loop method using PMA and various variable fidelity methods are given in Table 3. The table also includes the results from a standard RBDO method using just the high fidelity model.

Table 3. VF-RBDO double-loop PMA results for the AEET problem.

Method	HF Fn Evals	LF Fn Evals	Iters	Rel Cost
Multiplicative Scaling				
1st Order	228	3726	23	1129
2nd Order, BFGS	163	5300	14	1203
2nd Order, SR1	178	6506	17	1421
Additive Scaling				
1st Order	256	3774	27	1206
2nd Order, BFGS	152	5298	13	1175
2nd Order, SR1	138	4592	12	1034
Adaptive Hybrid Scaling				
1st Order	183	2969	16	903
2nd Order, BFGS	144	5538	15	1191
2nd Order, SR1	105	3200	10	743
RBDO SQP	1932	-	25	4830

The initial design is shown in Figure 8a and has a lift coefficient of 2.11. The deterministic solution has a lift coefficient of 2.69 while the reliable design, shown in Figure 8b, has a lift coefficient of 2.51. All of the trials converged to the same solution. The results given in Table 3 show that the variable fidelity methods have significantly reduced the relative computational cost of design compared to the standard SQP approach. All of the 2nd order methods reduced the number of high fidelity function calls but had mixed results when comparing the overall relative costs. Multiplicative 2nd order and the hybrid second order BFGS methods were more expensive because of a large increase of low fidelity function calls required. If the computational cost gap were increased, the 2nd order methods would have become much more efficient in all cases. The adaptive methods performed the best overall; they had a lower cost than either of the multiplicative or additive methods for the 1st order and 2nd order SR1 scalings. The highest savings came from the hybrid 2nd order SR1 scaling. This method reduced the relative cost of finding a reliable design by 85%.

VII. Summary and Conclusions

Compared with standard deterministic design optimization methods, reliability based design problems tend to greatly increase the computation time and expense required to reach a converged solution. In this research variable fidelity methods were used to reduce the cost of reliability based design optimization. This combined variable fidelity reliability based design optimization approach was compared to standard reliability optimization using two design problems: a nonlinear analytic problem and a high lift airfoil design problem. In both of the demonstration problems the number of high fidelity function calls required was significantly reduced using VF-RBDO.

Many different types of scaling options exist when using the variable fidelity approach. There are two main types of scaling functions, multiplicative and additive, which can be combined into an adaptive hybrid

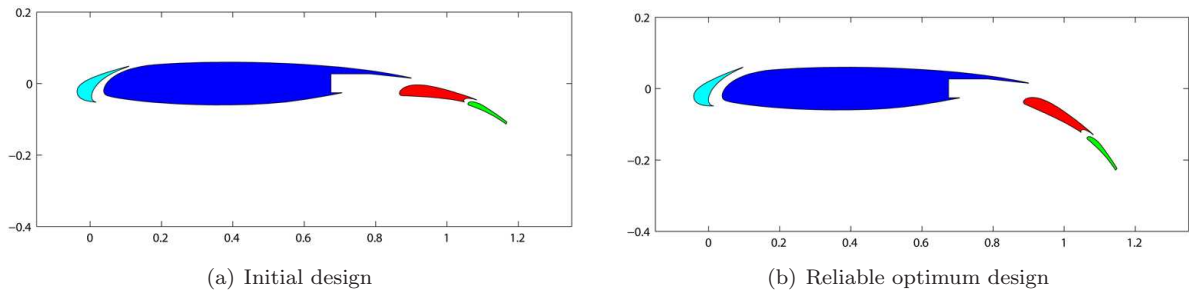


Figure 8. Initial and reliable optimum design configurations of the AEET.

method. Each of these scaling types can be approximated using first order or second order methods. In computing the Hessian, the second order methods use variable metric methods, BFGS and SR1, to reduce the computational expense. All of these options were also compared in the two demonstration problems. The second order variable fidelity scaling methods required a smaller number of high fidelity function calls compared to the first order models, but a penalty of an increase in low fidelity function calls was observed in some cases. The computational increase in low fidelity calls is usually offset by the savings in the high fidelity evaluations, but it is mainly dependent on the cost ratio between the two fidelity models. The results indicate that the additive method performs better than the multiplicative scaling for RBDO. The adaptive hybrid method was efficient at selecting the appropriate method without the designer having to select between the two scaling methods. In the airfoil design case the hybrid method actually had improved performance over either additive or multiplicative alone; however, these results are not true in general.

In conclusion, the VF-RBDO combined methodology has been shown to reduce the computational cost of performing reliability based design. The method requires a set of fidelity models and is most efficient when the relative cost between the models is large. Additionally, the variable fidelity and reliability based methods are easily combined.

Acknowledgments

This research effort was supported in part by the following grants and contracts: AFRL / DARPA / An-teon Corporation Contract F33615-98-D-3210, ONR Grant N00014-02-1-0786, and NSF Grant DMI-0114975.

References

- ¹Agarwal, H., Renaud, J. E., Lee, J. C., and Watson, L. T., "A Unilevel Method for Reliability Based Design Optimization," *Proceedings of the 45th AIAA/ASME/ASCE/AHS/ASC Structures, Structural Dynamics & Materials Conference*, No. AIAA 2004-2029, Palm Springs, CA, 19 - 22 Apr 2004 2004.
- ²Agarwal, H., Renaud, J. E., and Watson, L. T., "A Unilevel Architecture for Reliability Based Design Optimization," *Structural and Multidisciplinary Optimization*, 2004, pp. (Submitted For Review).
- ³Kuschel, N. and Rackwitz, R., "A New Approach for Structural Optimization of Series Systems," *Applications of Statistics and Probability*, Vol. 2, No. 8, 2000, pp. 987-994.
- ⁴Koch, P. N., Wujec, B., Golovidov, O., and Simpson, T. W., "Facilitating Probabilistic Multidisciplinary Design Optimization Using Kriging Approximation Models," *9th AIAA/USAF/NASA/ISSMO Symposium on Multidisciplinary Analysis and Optimization*, No. AIAA 2002-5602, 4-6 September 2002.
- ⁵Venkataraman, S., "Reliability Optimization of Structures Using Probabilistic Sufficiency Factor and Correction Response Surface," *Proceedings of the 45th AIAA/ASME/ASCE/AHS/ASC Structures, Structural Dynamics & Materials Conference*, No. AIAA 2004-2033, Palm Springs, CA, 19 - 22 Apr 2004 2004.
- ⁶Gano, S. E., Renaud, J. E., and Sanders, B., "Variable Fidelity Optimization Using a Kriging Based Scaling Function," *Proceedings of the 11th AIAA/ISSMO Multidisciplinary Analysis & Optimization Conference*, No. AIAA 2004-4460, Albany, NY, 30 August - 1 September 2004.
- ⁷Eldred, M. S., Giunta, A. A., Collis, S. S., Alexandrov, N. A., and Lewis, R. M., "Second-Order Corrections for Surrogate-

Based Optimization with Model Hierarchies,” *Proceedings of the 11th AIAA/ISSMO Multidisciplinary Analysis & Optimization Conference*, No. AIAA 2004-4457, Albany, NY, 30 August - 1 September 2004.

⁸Alexandrov, N. M., Lewis, R. M., Gumbert, C. R., Green, L. L., and Newman, P. A., “Optimization with variable-fidelity models applied to wing design,” *Proceedings of the 38th AIAA Aerospace Sciences Meeting and Exhibit*, No. AIAA 2000-0841, Reno, Nevada, 10-13 January 2000.

⁹Booker, A. J., Dennis, J. E., Frank, P. D., Serafini, D. B., Torczon, V., and Trosset, M. W., “A Rigorous Framework for Optimization of Expensive Function by Surrogates,” No. CRPC-TR98739-S, April 1998.

¹⁰Gano, S. E., Pérez, V. M., and Renaud, J. E., “Multi-Objective Variable-Fidelity Optimization of a Morphing Unmanned Aerial Vehicle,” *Proceedings of the 45th AIAA/ASME/ASCE/AHS/ASC Structures, Structural Dynamics & Materials Conference*, No. AIAA 2004-1763, Palm Springs, CA, 19 - 22 Apr 2004 2004.

¹¹Haldar, A. and Mahadevan, S., *Probability, Reliability and Statistical Methods in Engineering Design*, John Wiley & Sons, 2000.

¹²Rosenblatt, M., “Remarks on a Multivariate Transformation,” *The Annals of Mathematical Statistics*, Vol. 23, No. 3, September 1952, pp. 470-472.

¹³Brietung, K., “Asymptotic Approximations for Multinormal Integral,” *Journal of Engineering Mechanics*, Vol. 110, No. 3, 1984, pp. 357-366.

¹⁴Liu, P.-L. and Kiureghian, A. D., “Optimization Algorithms for Structural Reliability,” *Structural Safety*, Vol. 9, No. 3, 1991, pp. 161-177.

¹⁵Padmanabhan, D. and Batill, S. M., “Decomposition Strategies for Reliability Based Optimization in Multidisciplinary System Design,” *Proceedings of the 9th AIAA/USAF/NASA/ISSMO Symposium on Multidisciplinary Analysis & Optimization*, No. AIAA 2002-5471, Atlanta, GA, September 4-6 2002.

¹⁶Tu, J., Choi, K. K., and Park, Y. H., “A new study on Reliability-Based Design Optimization,” *Journal of Mechanical Design*, Vol. 121, December 1999, pp. 557-564.

¹⁷Polak, E., Wets, R. J.-B., and der Kiureghian, A., “On an Approach to Optimization Problems with a Probabilistic Cost and or Constraints,” *Nonlinear Optimization and Related Topics*, edited by G. D. Pillo and F. Giannessi, Vol. 36 of *Applied Optimization*, Kluwer Academic Publishers, 2000, pp. 299-316.

¹⁸Royset, J. O., Kiureghian, A. D., and Polak, E., “Reliability Based Optimal Structural Design by the Decoupling Approach,” *Reliability Engineering and System Safety*, Vol. 73, No. 3, 2001, pp. 213-221.

¹⁹Kirjner-Neto, C., Polak, E., and der Kiureghian, A., “An Outer Approximations Approach to Reliability-Based Optimal Design of Structures,” *Journal of Optimization Theory and Applications*, Vol. 98, No. 1, 1998, pp. 1-16.

²⁰Chen, W. and Du, X., “Sequential Optimization and Reliability Assessment Method for Efficient Probabilistic Design,” *ASME Design Engineering Technical Conferences and Computers and Information in Engineering Conference*, No. DETC2002/DAC-34127, Montreal, Canada, 2002.

²¹Chen, X. C., Hasselman, T. K., and Neill, D. J., “Reliability Based Structural Design Optimization For Practical Applications,” *Proceedings of the 38th AIAA/ASME/ASCE/AHS/ASC Structures, Structural Dynamics, and Materials Conference*, No. AIAA-97-1403, 1997, pp. 2724-2732.

²²Wang, L. and Kodiyalam, S., “An Efficient Method For Probabilistic and Robust Design With Non-Normal Distribution,” *Proceedings of the 43rd AIAA/ASME/ASCE/AHS/ASC Structures, Structural Dynamics, and Materials Conference*, No. AIAA 2002-1754, Denver, Colorado, April 22-25 2002.

²³Agarwal, H., Renaud, J. E., and Mack, J. D., “A Decomposition Approach for Reliability-Based Multidisciplinary Design Optimization,” *Proceedings of the 44th AIAA/ASME/ASCE/AHS/ASC Structures, Structural Dynamics, and Materials Conference & Exhibit*, No. AIAA 2003-1778, Norfolk, Virginia, April 7-10 2003.

²⁴Agarwal, H. and Renaud, J. E., “Decoupled methodology for Probabilistic Design Optimization,” *ASCE Joint Specialty Conference on Probabilistic Mechanics and Structural Reliability*, Albuquerque, NM, July 2004, (to be presented).

²⁵Alexandrov, N. M., Dennis, J. E., Lewis, R. M., and Torczon, V., “A Trust Region Framework for Managing the Use of Approximation Models in Optimization,” No. ICASE Report 97-50, NASA/CR-201745, 2001.

²⁶Alexandrov, N. M., Nielsen, E. J., Lewis, R. M., and Anderson, W. K., “First-Order Model Management with Variable-Fidelity Physics Applied to Multi-Element Airfoil Optimization,” No. AIAA paper 2000-4886, September 2000.

²⁷Conn, A. R., Gould, N. I. M., and Toint, P. L., “Global Convergence of a Class of Trust Region Algorithms for Optimization with Simple Bounds,” *SIAM Journal of Numerical Analysis*, Vol. 25, No. 2, 1988, pp. 433-464.

²⁸Giunta, A. A. and Eldred, M. S., “Implementation of a Trust Region Model Management Strategy in the DAKOTA Optimization Toolkit,” No. AIAA-2000-4935, 2000.

²⁹Rodríguez, J. F., Pérez, V. M., Padmanabhan, D., and Renaud, J. E., “Sequential Approximate Optimization Using Variable Fidelity Response Surface Approximations,” *Structural and Multidisciplinary Optimization*, Vol. 22, 2001, pp. 24-34, Published by Springer-Verlag.

³⁰Rodríguez, J. F. and Renaud, J. E., “Convergence of Trust Region Augmented Lagrangian Methods Using Variable Fidelity Approximation Data,” *Structural Optimization*, Vol. 15, 1998, pp. 141-156.

³¹Conn, A. R., Gould, N. I. M., and Toint, P. L., *Trust-Region Methods*, Society for Industrial and Applied Mathematics and Mathematical Programming Society, 2000.

³²Alexandrov, N. M. and Lewis, R. M., “First-Order Approximation and Model Management in Optimization, in Large-Scale PDE-Constrained Optimization,” *Springer-Verlag*, 2001.

³³Chang, K. J., Haftka, R. T., Giles, G. L., and Kao, P.-J., “Sensitivity-based Scaling for Approximating Structural Response,” *Journal of Aircraft*, Vol. 30(2), March-April 1993, pp. 283-288.

³⁴Lewis, R. M. and Nash, S. G., “A Multigrid Approach to the Optimization of Systems Governed by Differential Equations,” No. AIAA-2000-4890, 2000.

³⁵Broyden, C. G., “The Convergence of a Class of Double-rank Minimization Algorithms,” *J. Inst. Maths. Applics.*, Vol. 6, 1970, pp. 76-90.

- ³⁶Fletcher, R., "A New Approach to Variable Metric Algorithms," *Computer Journal*, Vol. 13, 1970, pp. 317–322.
- ³⁷Goldfarb, D., "A Family of Variable Metric Updates Derived by Variational Means," *Mathematics of Computing*, Vol. 24, 1970, pp. 23–26.
- ³⁸Shanno, D. F., "Conditioning of Quasi-Newton Methods for Function Minimization," *Mathematics of Computing*, Vol. 24, 1970, pp. 647–656.
- ³⁹Agarwal, H., Renaud, J. E., and Pérez, V. M., "Homotopy Methods for Constraint Relaxation in Unilevel Reliability Based Design Optimization," *Proceedings of the 11th AIAA/ISSMO Multidisciplinary Analysis & Optimization Conference*, No. AIAA 2004-4402, Albany, NY, 30 August - 1 September 2004.
- ⁴⁰Pérez, V. M. and Eldred, M. S., "Solving the infeasible Trust-region Problem Using Approximations," *Proceedings of the 11th AIAA/ISSMO Multidisciplinary Analysis & Optimization Conference*, No. AIAA 2004-4312, Albany, NY, 30 August - 1 September 2004.
- ⁴¹Padula, S. L. and Li, W., "Options for robust airfoil optimization under uncertainty," *9th AIAA/USAF/NASA/ISSMO Symposium on Multidisciplinary Analysis and Optimization*, No. AIAA 2002-5602, 4-6 September 2002.
- ⁴²Li, W., Huyse, L., and Padula, S. L., "Robust airfoil optimization to achieve drag reduction over a range of Mach numbers," *Structural and Multidisciplinary Optimization*, Vol. 24, No. 1, 2002, pp. 38–50.
- ⁴³Huyse, L., Padula, S. L., Lewis, R. M., and Li, W., "A probabilistic approach to free-form airfoil shape optimization under uncertainty," *AIAA Journal*, Vol. 40, No. 9, 2002, pp. 1764–1772.
- ⁴⁴Barnes, G. K., Master's thesis, The University of Texas, Austin, Texas, 1967.
- ⁴⁵Agarwal, H. and Renaud, J. E., "Reliability Based Design Optimization Using Response Surfaces in Application to Multidisciplinary Systems," *Engineering Optimization*, Vol. 36, No. 3, 2004, pp. 291–311.
- ⁴⁶MathWorks, *Optimization Toolbox For Use with MATLAB: User's Guide Version 3*, The MathWorks Inc, 2004.
- ⁴⁷Morgan, H. L. J., "Experimental Test Results of Energy Efficient Transport (EET) High-Lift Airfoil in Langley Low-Turbulence Pressure Tunnel," Tech. Rep. TM-2002-211780, NASA, Langley Research Center, Hampton Virginia, 2002.
- ⁴⁸Lin, J. C. and Dominik, C. J., "Parametric Investigation of a High Lift Airfoil at High Reynolds Numbers," *Journal of Aircraft*, Vol. 34, No. 4, 1997, pp. 485–491.
- ⁴⁹Gatlin, G. M. and McGhee, R. J., "Study of Semi-Span Model Testing Techniques," *Proceedings of the 14th Applied Aerodynamics Conference*, No. AIAA 96-2386, New Orleans, LA, 17-20 June 1996.
- ⁵⁰Anderson, W. K. and Bonhaus, D. L., "An Implicit Upwind Algorithm for Computing Turbulent Flows on Unstructured Grids," *Computers and Fluids*, Vol. 23, No. 1, 1994, pp. 1–21.
- ⁵¹Anderson, W. K., Rausch, R. D., and Bonhaus, D. L., "Implicit/Multigrid Algorithms for Incompressible Turbulent Flows on Unstructured Grids," *J. Comp. Phys.*, Vol. 128, 1996, pp. 391–408.
- ⁵²Marcum, D. L., "Adaptive Unstructured Grid Generation for Viscous Flow Applications," *AIAA Journal*, Vol. 34, No. 11, 1996, pp. 2440.
- ⁵³Marcum, D. L., "Advancing-Front/Local-Reconnection (AFLR) Unstructured Grid Generation," *Computational Fluid Dynamics Review*, 1998.